INT. J. REMOTE SENSING, 1998, VOL. 19, NO. 16, 3127–3140

# AVHRR temporal analysis of a savanna site in Brazil

H. FRANÇA and A. W. SETZER
INPE/DSR, C. Postal 515, 12201 S.J. Campos, SP, Brazil

(*Received 20 November 1996; in final form 24 November 1997*)

**Abstract.** This work investigated the temporal monitoring of savanna ('cerrado') vegetation phenology in the Emas National Park of Brazil utilizing 1.1 km full resolution daily images of the Advanced Very High Resolution Radiometer (AVHRR) on-board the NOAA-11 satellite. For a period of 18 months studied in 1992–93, only 26 images had useful data. Digital analysis of individual images concentrated on five sub-areas of up to 30 $km^2$ each. Channels used were 1 (0.6–0.7 $\mu$m), 2 (0.7–1.1 $\mu$m) and 3 (3.5–3.9 $\mu$m), as well as the Vegetation Index (NDVI) which combines channels 1 and 2. A high resolution Thematic Mapper (TM) Landsat image and field work provided ground data to identify the vegetation types. Channel 3 and NDVI showed the strongest temporal response to phenological changes of the vegetation, while channels 1 and 2 presented high dependence on the off-nadir scan angle. The results indicated large variations in the daily AVHRR signal of channels 1 and 2 for the same area, regardless of vegetation changes. Regular monitoring of the $2 \times 10^6$ $km^2$ of Brazilian cerrados using AVHRR full 1.1 km resolution is recommended, particularly with the 3.7 $\mu$m band.

## 1. Introduction

Natural savannas, or 'cerrados', represent one of Brazil's main biomes, and formerly covered about $1.8 \times 10^6$ $km^2$ (Coutinho 1990 a), or 20% of the country's area. Little is known about the cerrados' biological diversity and ecology, and nevertheless they have been rapidly removed in the last decades; occupation occurred without environmental concerns, mainly to introduce soy bean crops and pastures. The cerrado devastation, according to Coutinho (1990 b), is far more advanced than that of the Amazon forest and only 1.5% of its area is in government conservation units, though with no effective management plans.

Most of the Brazilian cerrados strive in seasonal tropical weather (Nimer and Brandão 1989), with Köppen's type 'Aw' or 'Cwa' in the south. Average temperatures are in the 22–26° C range during the year and the total precipitation is between 1100 and 1600 mm, though with irregular distribution. Two very distinct seasons predominate: a rainy summer, from October to April, with 90% of the annual rainfall and an average temperature of 22–28° C; and a dry winter, from May to September, with temperatures of about 16–24° C. Average maxima in spring and summer are in the 30–36° C range, while average winter minima reach the 6–16° C range.

Regarding the vertical structure of cerrado vegetation, two main types occur: woody with trees and shrubs, and grassy with herbaceous and undershrub plants. The proportion of each type determines the physiognomy of the cerrado type and five main distinct classes of cerrado are defined in the *lato* sense (Coutinho 1990 b). Ordered in biomass content above the ground, and also in height of the vegetation, they are: 'campo limpo' (open grasslands), 'campo sujo' (grasslands with intermediate

and sparse shrubs), 'campo cerrado' (open scrub to scattered medium trees), 'cerrado *stricto sensu*' (mixed vegetation with trees up to 7 m) and 'cerradão'. The latter is actually a forest with canopies of individual trees touching each other and a sparce understory herbaceous layer. The occurrence of different cerrado physiognomies follows changes in the soil physicochemical properties and also depend on the frequency of fire and the local climate (Goodland 1970, Eiten 1972). Natural fires are expected in intervals of many years.

Plants of the herbaceous undershrub type have superficial roots, not deeper than 20 cm, and suffer water stress during the dry season when above-ground parts dry and the leaves shed. For plants of the arboreous and shrub cerrados, the drying and shedding of leaves is not related to soil moisture since their roots reach up to 20 m in the soil, where moisture remains high even in the dry season (Coutinho 1990 a, 1990 b); for these plants the shedding of leaves in the May–September fall and winter seasons result mainly from the weather seasonality and the associated reduction in solar illumination.

Most orbital remote sensing studies of semiarid vegetation phenology are based on data from the Advanced Very High Resolution Radiometer (AVHRR) on-board the National Oceanographic and Atmospheric Administration (NOAA) series satellites; this results from the satellite's high temporal resolution of 1 day, and from a strong annual foliage cycle responding to a long and marked cloud-free dry season. Particularly used are the Normalized Difference Vegetation Index (NDVI) mosaic images, derived from the ratio of the difference between AVHRR channels 1 and 2 to their sum. Examples of this technique are found among others in the pioneering work of Tucker and Gatlin (1984) for the Nile River delta, in Justice *et al.* (1985) for many parts of the world, in Justice and Hiernaux (1986) for the Sahel of Niger, in Tucker *et al.* (1985) for Africa, in Justice *et al.* (1986) for east Africa, in Malingreau (1986) for Asia, and in Gutman (1990) for the USA. Phenolgy studies for Brazil based on AVHRR NDVI products have also been reported. Justice *et al.* (1985) showed strong NDVI yearly variations for the 'caatingas', or semiarid vegetation of the northeast; Assad *et al.* (1988) reported NDVI and precipitation relations for the cerrados of Minas Gerais, while Santos and Shimabukuro (1993) and Liu and Kogan (1996) analysed NDVI and precipitation for the cerrados of central Brazil in general.

These AVHRR phenology studies were based on mosaic images composed for many days, at spatial resolutions very different from the nominal sensor definition of 1.1 km. Mosaic image pixels present a mixed combination of averaging and sampling techniques of original pixels, resulting in an effective resolution of up to about 20 km as in the case of NOAA-GAC data resampled. Mosaics normally comprise a 15-day period, selecting the pixels with the highest NDVI in the images available in the period. Therefore, these NDVI composite images assemble averaged signals from neighbouring sites, under different conditions of solar illumination, imaging angles and tropospheric opacity.

In the present work we investigate the possibility of a phenology study in the Brazilian cerrados through AVHRR full raw resolution data. With this novel approach an attempt is made to refine currently used AVHRR-based techniques towards a more reliable interpretation of vegetation remote sensing.

## 2. Study area: the Emas National Park

The study area of this work is the Emas National Park (1320 $km^2$) located in the cerrado morphoclimatic zone of Brazil (Ab'Saber 1971), at an elevation between

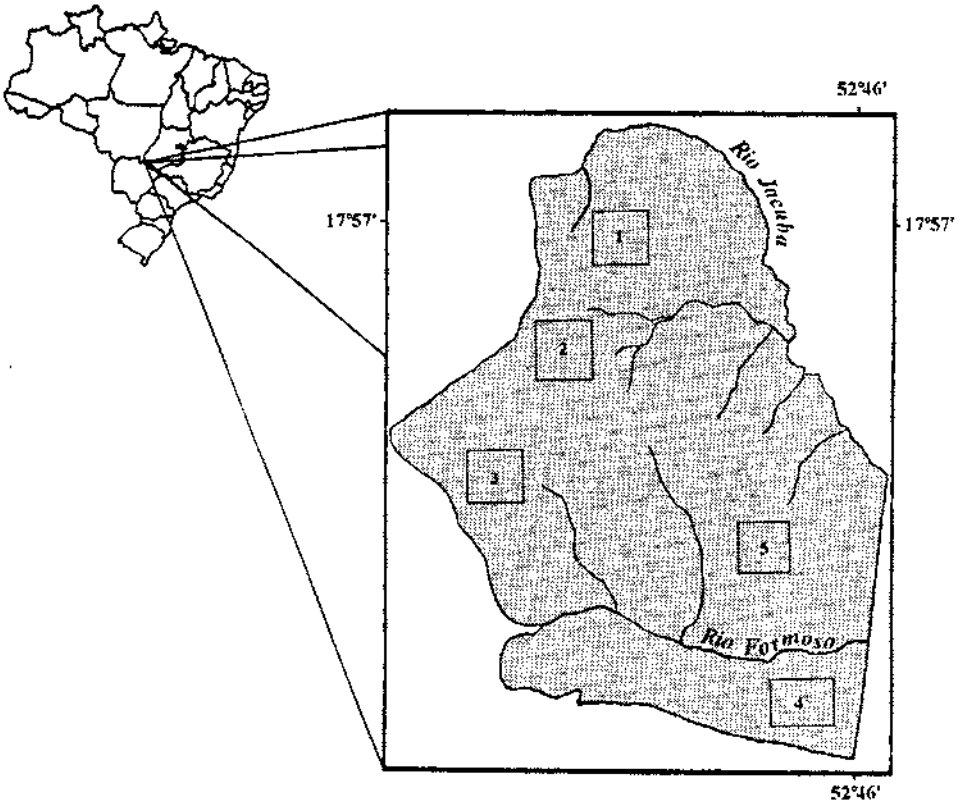


Figure 1. Location of the Emas National Park in Brazil and its five study areas.

650 and 900 m on the Brazilian central plateau, in the southwest of the Goiás state, Mineiros County, between 17° 49′ S and 18° 28′ S, and 52° 39′ W and 52° 10′ W (see figure 1). Its vegetation is characteristic of the cerrados, with campos limpos and campos sujos prevailing, where the grassy *Tristachya leiostachya* dominates (França 1994, Ramos-Neto and Machado 1996); gully forests, 'campo úmido' (swampy grass fields) and eutrophic seasonal tropical forests are also found. According to those responsible for the park in the Brazilian Environmental Institute, it is the most important conservation unit in the cerrados of Brazil because it is the largest one in this environment and, in addition, has undergone less anthropic action (IBAMA 1989). However, frequent and large arson fires within its limits (França and Setzer 1997) have to be considered when explaining the park's cerrado physiognomy.

## 3. Methodology

The methodology consisted of the temporal analysis of the AVHRR signal for typical cerrado vegetation to detect responses in the phenological and precipitation cycles. Unlike other AVHRR phenology studies, only individual images and not mosaics of degraded resolution were used.

### 3.1. *Sub-areas of study*

Five sub-areas of study, each about 20–30 $km^2$, were selected in the Emas National Park (see figure 1 for their location) representing the campos limpos and

campos sujos cerrado types; combined, these types correspond to about 80% of the park. The vegetation classes were initially determined from the analysis of a high resolution Landsat-5 satellite Thematic Mapper (TM) image, 'row/base' 224/73/B+, from 11 July 1993; a photographic colour print in the scale of 1:100 000 using channels 3 (0.63–0.69 $\mu$m), 4 (0.76–0.90 $\mu$m) and 5 (1.55–1.75 $\mu$m) was used. A field trip followed to corroborate the prevailing cerrado physiognomies present in each sub-area. The limits of the park and of the sub-areas were digitized using a Geographical Information System (GIS) and 1:100 000 scale topographic charts from IBGE (1977–78). None of these five sub-areas underwent fire during the study period, although other areas of the Park did burn; the study of the areas burned will be the subject of a future publication using similar methods.

3.2. *Selection and treatment of NOAA-11/AVHRR imagery*

The temporal analysis of the Emas National Park vegetation was carried out in digital images of the afternoon passes of the AVHRR aboard the NOAA-11 satellite, with 1.1 km nadir resolution (Kidwell 1993). The period studied covered 547 days, from 1 June 1992 to 30 November 1993, when images from 344 days were recorded by the Brazilian National Space Institute (INPE) receiving station located at C. Paulista, at about 22° 41′ S and 45° W. Channels 1 (0.6–0.7 $\mu$m), 2 (0.7–1.1 $\mu$m) and 3 (3.5–3.9 $\mu$m) were recorded at 8-bit resolution (256 grey-levels, or digital numbers (DNs)).

The images were initially screened regarding equatorial crossing and free cloud cover over the National Park. Only satellite crossings within the interval of 47°–63° W longitude were accepted, which kept the side-looking scan angle of AVHRR for the National Park between columns 394 and 1891 in any image (about 34° eastwards and 47° westwards from nadir). The images thus selected were next geometrically corrected to the cylindrical equidistant projection, and a sector of $101 \times 101$ pixels containing the study area was extracted for detailed exam.

Three prominent ground control points at the limits of the Emas National Park provided the references to co-register the study area and the five sub-areas in the AVHRR images. Channel 3 images were used for this purpose because of their better contrast in vegetation boundaries (Achard and Estreguil 1995, Di Maio-Mantovani and Setzer 1996 a, 1996 b). The individual sub-areas represented homogeneous cerrado types and had 20–30 pixels (see figure 1).

The analysis of the temporal response of the vegetation was based on the variation of the average value of the DNs of the AVHRR pixels in each of the five sub-areas in the individual images. For channels 1 and 2 these average values were converted to radiance using the satellite calibration curves (Kidwell 1993), and compensated for the sun elevation angle and earth–sun distance during image acquisition. Next, the radiances were converted back to DNs using the same calibration curves. For channel 3 images, only the earth–sun distance correction was applied. Also calculated for each sub-area was the NDVI obtained from the corrected DNs and following well-established procedures (Kidwell 1990). Daily records of precipitation were also used to interpret the satellite information. The closest meteorological station found was at Jataí, about 120 km north-east of the National Park (França 1994).

No atmospheric correction was made in the imagery. The region is subject to large variations in atmospheric opacity in the dry season caused by smoke from vegetation fires in the area. Since data showing these variations during AVHRR image acquisition does not exist for the site under analysis, any attempt to correct

such effects would be highly uncertain. For example, at Cuiaba, located 250 km north-west of the study area, and also in a cerrado environment, the atmospheric optical thickness varied from 0.4 to 2.8 in the fire season of 1993, with significant day-to-day oscillations (Holben *et al.* 1996).

## 4. Results and discussion

Of the 344 AVHRR images available only 26, or 7.5% of the total, had no or minor cloud cover over the study area and these were selected for the temporal analysis (see table 1). Just three images could be selected during the wet period, from November to April; in addition, five images could not be fully used because of small local clouds. Therefore, although the daily image acquisition frequency of AVHRR was adequate for a phenological study, actual data imposed strong limitations, particularly in the rainy period. The AVHRR images in the text are referred to as 'En', where 'n' corresponds to 1–26 according to their acquisition sequence. Further details of the images and data can be found in França (1994).

### 4.1. *AVHRR Channel 1 (0.58–0.68 μm) results*

Table 2 summarizes the DNs of AVHRR channel 1 for the five sub-areas studied in the 26 images analysed. The lowest and highest averaged DNs were 24.4 (5.5% albedo) for E25 and 41.3 (11.9% albedo) for E6, with higher values corresponding to off-nadir imaging of the Emas National Park (see figure 2 and table 2, channel 1).

The variation in the signal caused by the increase in the slant angle is evident in the sequence of images E14, E15 and E16, of the 1993 Julian days 175, 176 and 177, respectively. Since these are consecutive days, when no rains, frosts or fires occurred,

Table 1. AVHRR images used between 1 June 1992 and 31 November 1993. ND, total number of days; NR, number of non-recorded images; NE, number of images with Emas National Park on the edge; NP, number of images with bad recording; NU, number of potentially useful images; NC, number of images with Emas National Park under clouds; UI, number of useful images.

| Date | ND | NR | NE | NP | NU | NC | UI |
|---|---|---|---|---|---|---|---|
| June 92 | 30 | 2 | 6 | 4 | 18 | 14 | 4 |
| July 92 | 31 | — | 6 | 1 | 24 | 19 | 5 |
| Aug 92 | 31 | 2 | 8 | 2 | 19 | 19 | — |
| Sep 92 | 30 | 1 | 7 | 1 | 21 | 19 | 2 |
| Oct 92 | 31 | 2 | 8 | — | 21 | 21 | — |
| Nov 92 | 30 | 4 | 7 | 2 | 17 | 17 | — |
| Dec 92 | 31 | 2 | 7 | 3 | 19 | 19 | — |
| Jan 93 | 31 | 18 | 3 | 2 | 8 | 8 | — |
| Feb 93 | 28 | 13 | 5 | — | 10 | 10 | — |
| Mar 93 | 31 | 8 | 9 | 2 | 12 | 12 | — |
| Apr 93 | 30 | 4 | 7 | 3 | 16 | 15 | 1 |
| May 93 | 31 | 11 | 7 | — | 13 | 13 | — |
| June 93 | 30 | 1 | 7 | — | 22 | 19 | 4 |
| July 93 | 31 | 1 | 8 | — | 22 | 16 | 6 |
| Aug 93 | 31 | 4 | 7 | — | 20 | 18 | 2 |
| Sep 93 | 30 | — | 9 | — | 21 | 21 | — |
| Oct 93 | 31 | 6 | 6 | 1 | 18 | 16 | 2 |
| Nov 93 | 30 | 1 | 7 | 1 | 21 | 21 | — |
| Total | 548 | 80 | 124 | 22 | 322 | 297 | 26 |
| % of total | 100 | 14.6 | 22.6 | 4.0 | 58.9 | 54 | 4.7 |

Table 2. Grey-level (DN) averages for the five sample areas of the Emas National Park in the 26 AVHRR images (E1–E26) used in the study.

| Year | Image | Day | A1 | A2 | A3 | A4 | A5 | Ave. | Year | Image | Day | A1 | A2 | A3 | A4 | A5 | Ave. |
|---|---|---|---|---|---|---|---|---|---|---|---|---|---|---|---|---|---|
| **Channel 1** | E1 | 152 | 29·4 | — | 29·6 | — | — | 29·5 | **Channel 3** | E1 | 152 | 140·3 | — | 138·3 | — | — | 139·3 |
| *1992* | E2 | 153 | 27·8 | 26·5 | 27·1 | 26·1 | 26·1 | 26·7 | *1992* | E2 | 153 | 136·7 | 134·7 | 136·3 | 133·6 | 135·9 | 135·4 |
| | E3 | 159 | 36·9 | 35·2 | 35·4 | 35·0 | 35·9 | 35·7 | | E3 | 159 | 135·8 | 135·8 | 135·3 | 132·4 | 135·1 | 134·9 |
| | E4 | 167 | — | — | — | 35·9 | 38·5 | 37·2 | | E4 | 167 | — | — | — | 140·1 | 139·9 | 140·0 |
| | E5 | 186 | 29·0 | 28·4 | 29·0 | — | — | 28·8 | | E5 | 186 | 125·3 | 122·5 | 120·5 | — | — | 122·7 |
| | E6 | 200 | 42·5 | 40·7 | 41·9 | 39·6 | 41·8 | 41·3 | | E6 | 200 | 137·2 | 136·0 | 134·0 | 136·5 | 137·1 | 136·1 |
| | E7 | 201 | 35·2 | 35·1 | 35·1 | 34·6 | 35·0 | 35·0 | | E7 | 201 | 126·3 | 123·6 | 124·2 | 124·3 | 123·7 | 124·4 |
| | E8 | 205 | 39·4 | 39·2 | 39·6 | 40·5 | 39·3 | 39·6 | | E8 | 205 | 131·1 | 129·4 | 128·3 | 130·5 | 130·3 | 129·9 |
| | E9 | 211 | 29·8 | 29·5 | 29·5 | 29·5 | 29·5 | 29·5 | | E9 | 211 | 111·6 | 106·8 | 105·8 | 106·1 | 107·6 | 107·6 |
| | E10 | 251 | 33·7 | 33·2 | 33·1 | 32·3 | 32·0 | 32·8 | | E10 | 251 | 108·6 | 105·0 | 104·1 | 110·1 | 107·9 | 107·1 |
| | E11 | 252 | 29·0 | 29·6 | 29·1 | 28·6 | 30·7 | 29·4 | | E11 | 252 | 100·5 | 95·7 | 95·0 | 98·9 | 100·1 | 98·1 |
| *1993* | E12 | 117 | 27·7 | 33·5 | 27·2 | 31·0 | 27·8 | 28·4 | *1993* | E12 | 117 | 138·8 | — | 139·6 | 140·8 | 138·5 | 139·4 |
| | E13 | 174 | 30·5 | 30·2 | 30·3 | 30·2 | 30·2 | 30·3 | | E13 | 174 | 145·3 | 144·5 | 145·4 | 144·0 | 145·0 | 144·8 |
| | E14 | 175 | — | 30·8 | 30·8 | — | 30·7 | 30·8 | | E14 | 175 | — | 143·7 | 144·0 | — | 141·2 | 143·0 |
| | E15 | 176 | 32·0 | 32·3 | 32·4 | 31·5 | 33·9 | 32·4 | | E15 | 176 | 137·5 | 138·3 | 138·7 | 138·2 | 138·8 | 138·3 |
| | E16 | 177 | 37·1 | 37·0 | 37·1 | 36·8 | 37·1 | 37·0 | | E16 | 177 | 135·7 | 135·9 | 136·1 | 135·1 | 135·3 | 135·6 |
| | E17 | 183 | 30·6 | 30·9 | 31·0 | 30·4 | 30·8 | 30·7 | | E17 | 183 | 137·5 | 136·6 | 136·5 | 133·7 | 136·1 | 136·1 |
| | E18 | 185 | 34·4 | 34·7 | 35·8 | 34·6 | 34·6 | 34·8 | | E18 | 185 | 128·1 | 127·6 | 126·9 | 126·2 | 126·7 | 127·1 |
| | E19 | 191 | 30·8 | 31·0 | 31·0 | 31·0 | 31·0 | 31·0 | | E19 | 191 | 135·8 | 134·8 | 135·0 | 133·8 | 134·7 | 134·8 |
| | E20 | 192 | 31·3 | 31·2 | 31·5 | — | 31·4 | 31·3 | | E20 | 192 | 133·4 | 133·4 | 134·0 | — | 132·9 | 133·4 |
| | E21 | 198 | 38·3 | 38·0 | 37·8 | 39·5 | 37·9 | 38·3 | | E21 | 198 | 139·7 | 138·3 | 138·4 | 137·0 | 137·6 | 138·2 |
| | E22 | 201 | 32·1 | 31·8 | 33·4 | 31·8 | 31·8 | 32·2 | | E22 | 201 | 127·3 | 127·2 | 127·0 | 126·3 | 126·9 | 127·0 |
| | E23 | 216 | 31·1 | 30·8 | 31·4 | 31·0 | 31·1 | 31·1 | | E23 | 216 | 119·8 | 118·6 | 118·5 | 118·7 | 119·5 | 119·0 |
| | E24 | 218 | 38·5 | 38·1 | 38·5 | 36·4 | 36·9 | 37·7 | | E24 | 218 | 115·0 | 112·9 | 114·0 | 113·7 | 113·7 | 113·9 |
| | E25 | 280 | 24·4 | 24·3 | 24·3 | 24·4 | 24·3 | 24·4 | | E25 | 280 | 107·8 | 128·9 | 127·2 | 130·8 | 129·5 | 124·8 |
| | E26 | 281 | 28·4 | 25·2 | 26·6 | 27·3 | 26·7 | 26·8 | | E26 | 281 | 93·6 | 117·0 | 114·9 | 116·7 | 115·7 | 111·6 |

| | | | | | | | | | | | | | | | | | | |
|---|---|---|---|---|---|---|---|---|---|---|---|---|---|---|---|---|---|---|
| **Channel 2** | E1 | 152 | 49·3 | — | 48·1 | — | — | 48·7 | **NDVI** | E1 | 152 | 0·25 | — | 0·24 | — | — | 0·25 |
| *1992* | E2 | 153 | 49·6 | 46·9 | 46·5 | 47·1 | 46·6 | 47·3 | *1992* | E2 | 153 | 0·28 | 0·28 | 0·26 | 0·29 | 0·28 | 0·28 |
| | E3 | 159 | 61·6 | 59·3 | 59·1 | 56·5 | 58·8 | 59·1 | | E3 | 159 | 0·25 | 0·26 | 0·25 | 0·23 | 0·24 | 0·25 |
| | E4 | 167 | — | — | — | 58·5 | 60·5 | 59·5 | | E4 | 167 | — | — | — | 0·24 | 0·22 | 0·23 |
| | E5 | 186 | 46·0 | 43·4 | 44·4 | — | — | 44·6 | | E5 | 186 | 0·23 | 0·21 | 0·21 | — | — | 0·16 |
| | E6 | 200 | 58·7 | 56·7 | 56·2 | 56·5 | 56·2 | 56·9 | | E6 | 200 | 0·16 | 0·16 | 0·15 | 0·18 | 0·15 | 0·16 |
| | E7 | 201 | 49·5 | 48·1 | 48·1 | 47·6 | 47·7 | 48·2 | | E7 | 201 | 0·17 | 0·16 | 0·16 | 0·16 | 0·15 | 0·16 |
| | E8 | 205 | 52·0 | 50·2 | 51·0 | 50·3 | 49·9 | 50·7 | | E8 | 205 | 0·14 | 0·12 | 0·13 | 0·11 | 0·12 | 0·12 |
| | E9 | 211 | 43·3 | 42·1 | 42·3 | 41·6 | 41·1 | 42·1 | | E9 | 211 | 0·19 | 0·18 | 0·18 | 0·17 | 0·16 | 0·18 |
| | E10 | 251 | 43·5 | 41·4 | 42·7 | 42·6 | 42·3 | 42·5 | | E10 | 251 | 0·13 | 0·11 | 0·13 | 0·14 | 0·14 | 0·13 |
| | E11 | 252 | 40·9 | 40·6 | 40·7 | 40·5 | 40·0 | 40·5 | | E11 | 252 | 0·17 | 0·16 | 0·17 | 0·17 | 0·13 | 0·16 |
| *1993* | E12 | 117 | 46·3 | — | 43·8 | 50·6 | 46·2 | 46·8 | *1993* | E12 | 117 | 0·25 | — | 0·23 | 0·24 | 0·25 | 0·24 |
| | E13 | 174 | 46·2 | 46·2 | 46·2 | 46·2 | 46·2 | 46·2 | | E13 | 174 | 0·21 | 0·21 | 0·21 | 0·21 | 0·21 | 0·21 |
| | E14 | 175 | — | 41·3 | 42·0 | — | 42·1 | 41·8 | | E14 | 175 | — | 0·14 | 0·15 | — | 0·16 | 0·15 |
| | E15 | 176 | 46·3 | 44·2 | 45·0 | 44·8 | 46·4 | 45·3 | | E15 | 176 | 0·18 | 0·15 | 0·16 | 0·17 | 0·16 | 0·17 |
| | E16 | 177 | 54·9 | 52·0 | 53·2 | 51·4 | 53·5 | 53·0 | | E16 | 177 | 0·19 | 0·17 | 0·18 | 0·17 | 0·18 | 0·18 |
| | E17 | 183 | 41·8 | 41·5 | 42·1 | 43·0 | 41·9 | 42·0 | | E17 | 183 | 0·15 | 0·15 | 0·15 | 0·17 | 0·15 | 0·16 |
| | E18 | 185 | 50·2 | 48·5 | 50·2 | 47·8 | 50·2 | 49·4 | | E18 | 185 | 0·19 | 0·17 | 0·17 | 0·16 | 0·18 | 0·17 |
| | E19 | 191 | 41·7 | 41·2 | 41·5 | 41·5 | 41·5 | 41·5 | | E19 | 191 | 0·15 | 0·14 | 0·14 | 0·14 | 0·14 | 0·15 |
| | E20 | 192 | 42·8 | 41·8 | 42·5 | — | 43·6 | 42·7 | | E20 | 192 | 0·16 | 0·15 | 0·15 | — | 0·16 | 0·15 |
| | E21 | 198 | 50·4 | 49·1 | 46·7 | 50·7 | 50·4 | 49·5 | | E21 | 198 | 0·14 | 0·13 | 0·11 | 0·12 | 0·14 | 0·13 |
| | E22 | 201 | 44·9 | 43·9 | 44·7 | 44·9 | 45·1 | 44·7 | | E22 | 201 | 0·17 | 0·16 | 0·15 | 0·17 | 0·17 | 0·16 |
| | E23 | 216 | 40·3 | 39·9 | 40·3 | 40·3 | 40·2 | 40·2 | | E23 | 216 | 0·13 | 0·13 | 0·12 | 0·13 | 0·13 | 0·13 |
| | E24 | 218 | 48·3 | 47·0 | 47·8 | 47·2 | 47·9 | 47·6 | | E24 | 218 | 0·11 | 0·10 | 0·11 | 0·13 | 0·13 | 0·12 |
| | E25 | 280 | 30·8 | 36·4 | 36·8 | 39·5 | 35·9 | 35·9 | | E25 | 280 | 0·12 | 0·20 | 0·20 | 0·24 | 0·19 | 0·19 |
| | E26 | 281 | 39·9 | 45·4 | 45·0 | 47·6 | 44·1 | 44·4 | | E26 | 281 | 0·17 | 0·29 | 0·26 | 0·27 | 0·25 | 0·25 |

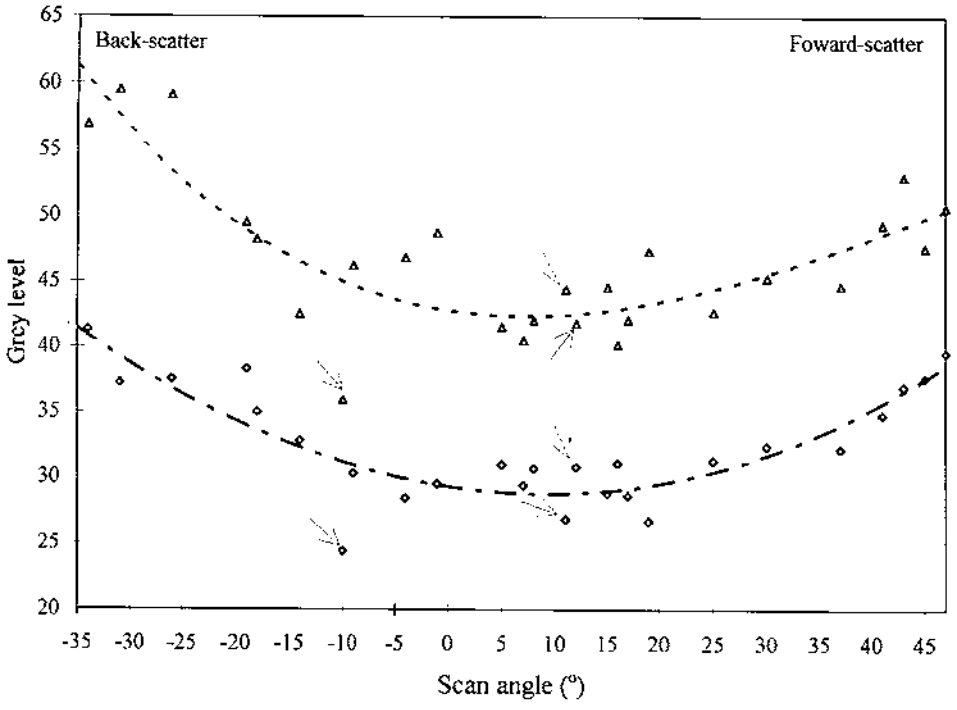


Figure 2. Effect of the AVHRR scan angle on the grey-level (DNs) of channels 1 (◇ symbols) and 2 (△ symbols). Arrows indicate the three images in the wet season, and the curves represent second-order polynomial fits to the two data sets.

the general reflective properties of the vegetation can be assumed to remain constant in such a short period. However, the averaged DNs increased progressively from 30.8 (7.9% albedo) to 32.8 (8.7% albedo) and to 37.0 (10.3% albedo). This was interpreted as a result of the increase in the AVHRR viewing angle: on the first image E14, the National Park was on column 1243 (11.9° off-nadir), very close to the nadir column 1048, while on E15 the column was 1576 (29.9° off-nadir) and on E16 1812 (42.6° off-nadir). In this case, the eastward shift of about 3.1° of longitude per day in the satellite relative position caused an increase in the forward scattering radiation, thus also augmenting the signal reaching the AVHRR. As seen in figure 2, it is important to notice that this signal increase is about one-third of the total channel 1 variation observed in the full sequence of images.

Very similar results also were observed in the other daily sequences of images, E1–E2, E6–E7 and E10–E11 (see table 2). This off-nadir effect agrees with the data of Kimes (1983) and Kimes *et al.* (1984) who reported an increase in the signal of AVHRR channel 1 for off-nadir angles, which in itself was stronger for exposed soils in comparison to soils partially covered with vegetation.

The effects of back and forward scattering in channel 1 data are depicted in figure 2, where DNs were plotted against the satellite scan angle. A second-order polynomial curve was fitted to the 26 data points in order to show the general variation pattern found for this set of measurements.

To reduce the off-nadir viewing effect just described, only channel 1 images with the National Park within $\pm 15°$ from the nadir were used in the temporal analysis.

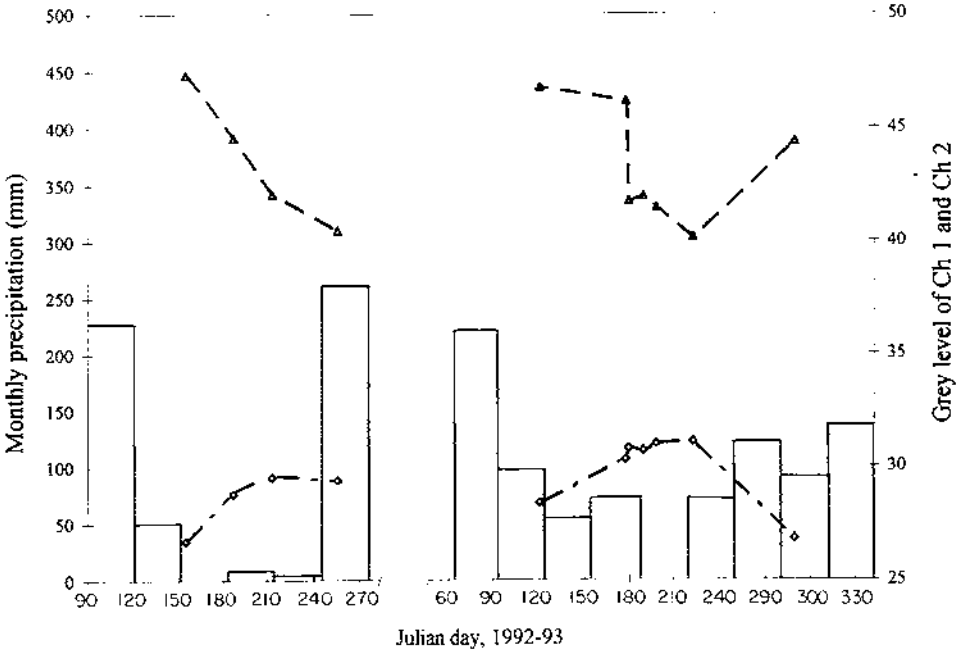


Figure 3. Temporal variation of grey-level (DNs) for AVHRR channels 1 (◇ symbols) and 2 (△ symbols) at the Emas National Park and monthly precipitation.

These 11 images presented the averaged lowest and highest DNs of 26.7 (6.3% albedo) and 30.8 (7.9% albedo), with a variation of 15.4% in the signal, or 25.4% in albedo. Figure 3 shows the increase in DNs along the advance of the dry seasons of 1992 and 1993, as well as the decrease at the end and beginning of the wet seasons, with an inverse response to the monthly precipitation curve.

4.2. *AVHRR Channel 2 (0.72–1.1 μm) results*

The variation of the DN levels in channel 2 for the five sub-areas was higher than that of channel 1, with average lowest and highest DNs of 35.9 (11.6% albedo) for E25 and 59.5 (21.7% albedo) for E4 (see table 2, channel 2). As in channel 1, strong variations related to the AVHRR viewing angle were found, and particularly high DNs occurred in the off-nadir images of the Emas National Park. In the image sequence of the consecutive days E14–E15–E16, the increase in signal with the off-nadir angle is also evident, as in channel 1 (see figure 2 and table 2). In this particular sequence, the difference of 11.4 DNs is about half of the total DN range for the complete set of data in channel 2. The other image sequences of successive or very close days, E6–E7, E10–E11, E19–E20, E23–E24, also presented an increase in the signal strength with the off-nadir angle. The overall effect of back and forward scattering in channel 2 is suggested in figure 2 through the second-order polynomial fit; a similar shape to that found for the channel 1 fit is noticeable.

As with channel 1, only 11 images with the National Park within $\pm 15°$ off-nadir were used in figure 3. The five sub-areas had an average minimum DN of 40.2 (13.5% albedo) and an average maximum DN 47.3 (16.5% albedo), corresponding to a variation of 17.7% in the sensor signal, or 22.2% in albedo. For both years of

data the DNs presented a reduction towards the dry season, following the pattern of the precipitation curve.

4.3. *AVHRR Channel 3 (3.55–3.93 μm) results*

DN average values for channel 3 in the study area were in the range of 98.1–144.8 as seen in table 2, with a variation of 47.6%, or 18.2% of the sensor radiometric range. Apparently, as seen in the polynomial fit of figure 4, these measurements were not influenced by the AVHRR scanning angle.

The band of channel 3 measures earth-emitted and sun-reflected energy, although sun glint from water and exposed soils may occasionally overcome the emitted signal (Setzer and Veerstrate 1994). Its original grey-scale is naturally inverted to facilitate interpretation of clouds, so high DNs refer to low temperature and appear as white tones in the image, while low DNs refer to high temperatures and appear as dark tones. Applications of daytime images of channel 3 to vegetation studies are rare and point to its strong potential, although with constraints (Amaral 1992, Kaufman and Remer 1994, Achard and Estreguil 1995, Di Maio-Mantovani and Setzer 1996 a, 1996 b).

The temporal variation of channel 3 for the Emas National Park responded to seasonal variations of the cerrados but in an unexpected way if only an emitted thermal signal is considered. As depicted in figure 5, the DNs decreased (higher 'temperatures') as the dry season progressed and increased (lower 'temperatures') in the beginning and end of the rainy period. Since the dry season occurs in the winter and therefore is colder than the wet season, the signal of channel 3 must have had

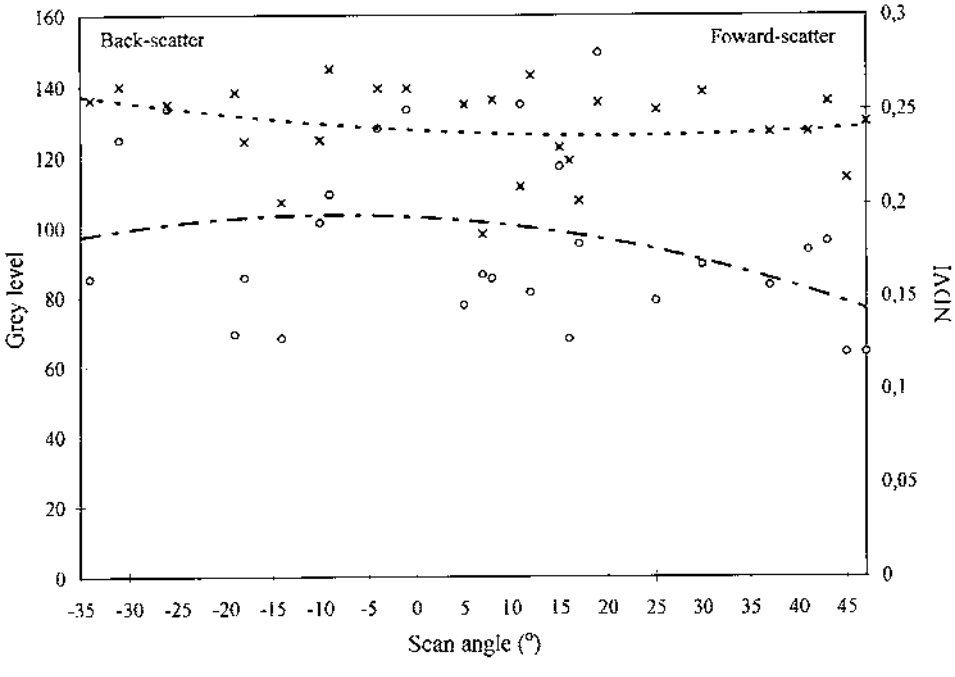


Figure 4. Effect of the AVHRR scan angle on the grey-level (DNs) of channels 3 (× symbols) and NDVI (○ symbols). The curves represent second-order polynomial fits to the two data sets.

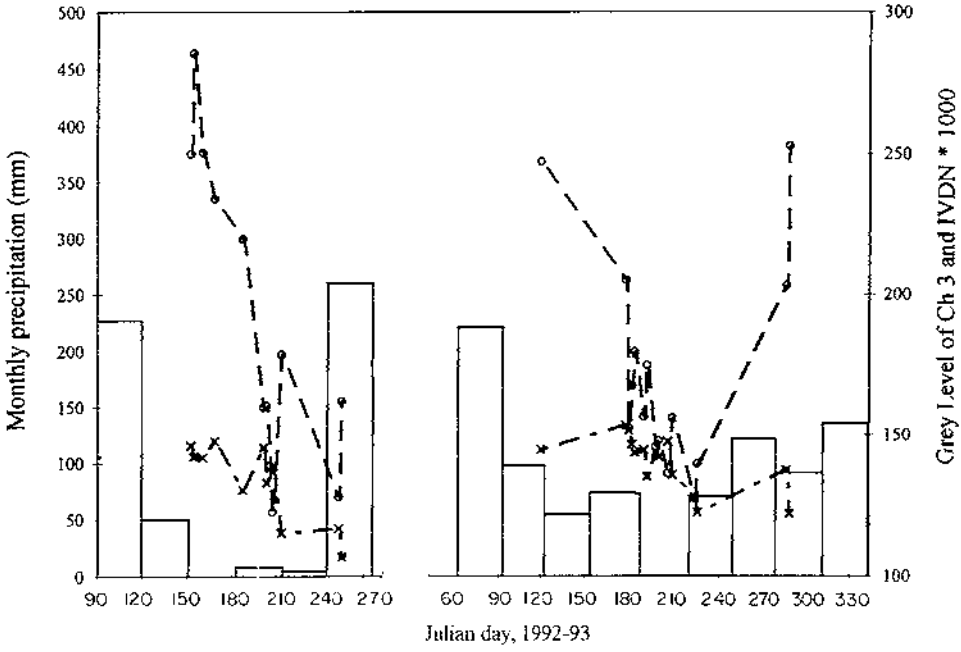


Figure 5. Temporal variation of grey-level (DNs) for AVHRR channels 3 (× symbols) and NDVI (○ symbols) at the Emas National Park and monthly precipitation.

an opposite response in relation to what was observed. This behaviour can be accounted for if a significant reflected component is also assumed, increasing in the dry season when the dry vegetation and partially exposed soils reflect more sunlight. Inversely, in the wet season, darker and sprouting vegetation with higher moisture content covering the soil reduced the reflection of sunlight, indicating lower temperatures.

Therefore, channel 3 responded more markedly to the seasonality or water stress of the cerrados than the other AVHRR channels. The observed lack of atmospheric effects on the viewing angle, a highly desired characteristic in remote sensing, is most certainly a consequence of the little effect smoke aerosols have in the 3.7 $\mu$m band (Kaufman and Remer 1994).

### 4.4. *NDVI results*

The NDVI temporal data for the Emas National Park is presented in table 2 and figure 5; they varied from 0.12 to 0.28, or 133%, which corresponds to 16% in its range of 0–1. Some unexpected variations of the NDVI, as in the sequence of days 174–177 in 1993 (images E13–E14–E15–E16) shown in figure 5, did not depend on actual changes in the vegetation cover. A decrease in NDVI caused by forward-scattering is evident in the curve fit of figure 4 (lower curve), although with a large spread of data around the curve; NDVI varied much less with the scanning angle than channels 1 and 2 (figure 2), in agreement with the reports of Kimes (1983) and Kimes *et al.* (1984).

In general, as seen in figure 5, the NDVI response in the individual images followed the temporal changes of the vegetation, with decreasing values in the dry season and increases in the rainy season. These variations indicate the effect of the

Table 3.

| | Channel 1 | Channel 2 | Channel 3 | NDVI |
|---|---|---|---|---|
| Signal variation | 15% | 18% | 48% | 133% |
| Range in the scale | 2% | 3% | 18% | 16% |

water stress in a long dry season and are similar to the variations found in the NDVI studies for the African Sahel reviewed by Prince *et al.* (1990).

The similar behaviour of the NDVI and channel 3 data observed in figure 5 should be stressed. A similar result can be found in D'Souza and Malingreau (1994) in their AVHRR analysis of largely deforested areas over the Rondonia state in Brazil.

## 5. Conclusions

Using a test site this work showed that the phenology of Brazilian cerrados can be followed and studied to some extent using AVHRR channels 1, 2, 3, and also the NDVI combination of channels 1 and 2, all with 1.1 km resolution. An unusually high occurrence of cloud cover limited the number of useful images, particularly in the wet season, but did not preclude the study.

Data from channels 1 and 2 were limited to $\pm 15^{\circ}$ near-nadir imaging and indicated seasonal changes only to a minor extent when compared to channel 3 and NDVI. These last two, in addition to a stronger seasonal signal variation, were much less dependent on the AVHRR scanning angle. Attention is called to the use of channel 3 (3.5–3.9 $\mu$m) in vegetation and phenology studies. In relation to the NDVI, the 3.7 $\mu$m band was much less sensitive to atmospheric effects (and scan angles) and presented no strong oscillation in intervals of a few days, when the vegetation signal remained constant. The comparative responses of the channels to the yearly phenological cerrado changes are summarized in table 3.

The regular use of AVHRR 1.1 km data is suggested to monitor the Brazilian cerrado with a dual purpose: phenology studies, and detection of the current intense and uncontrolled conversion to agricultural and pasture. Future satellite sensors with larger number of channels and more bands covered, such as MODIS/EOS, should bring improved spectral definition allowing even better phenology studies.

## Acknowledgments

The authors acknowledge the partial support of CNPq (grants 3315005-2 and 300557/97-3) and FAPESP (grant 93/1737-1), and also the collaboration of M. C. Pereira from DSR/INPE, DSA/INPE and LTID/INPE.

## References

Ab'Saber, A. N., 1971, A organização natural das paisagens inter e subtropicais brasileiras. *Simpósio sobre o cerrado*, 3, M. G. Ferri, editor (São Paulo: E. Blücher/Edusp), pp. 1–14.

Achard, F., and Estreguil, C., 1995, Forest classification of Southeast Asia using NOAA-AVHRR data. *Remote Sensing of Environment*, **54,** 198–208.

Amaral, S., 1992, *Imagens do sistema sensor AVHRR/NOAA na detecção e avaliação de desmatamentos na floresta amazônica—relações com dados do sistema TM/Landsat.* MSc thesis, Instituto Nacional de Pesquisas Espaciais—INPE, S. J. Campos (INPE-5501-TDI/516) (in Portuguese).

Assad, E., Setzer, A. W., and Moreira, L., 1988, Estimativa da precipitação através de Índices de Vegetação do Satélite NOAA. *Anais, V Simposio Brasileiro de Sensoriamento Remoto*, Natal, RN, (INPE, S. J. Campos), Vol. 2, pp. 425–429 (in Portuguese).

COUTINHO, L. M., 1990 a, O cerrado e a ecologia do fogo. *Ciência Hoje*, **12,** 22–30 (in Portuguese).

COUTINHO, L. M., 1990 b, Fire in the ecology of the Brazilian cerrado. *Fire in the Tropical Biota*, Ecological Studies, 84, edited by J. G. Goldammer (New York: Springer-Verlag), pp. 82–105.

DI MAIO-MANTOVANI, A., and SETZER, A. W., 1996 a, A change detection methodology for the amazon forest using multitemporal NOAA/AVHRR data and GIS—preliminary results. ASTM publication, STP-1279, pp. 43–46.

DI MAIO-MANTOVANI, A., and SETZER, A. W., 1996 b, Deforestation detection in the Amazon with an AVHRR-based system. *International Journal of Remote Sensing*, **18,** 273–286.

D'SOUZA, G., and MALINGREAU, J. P., 1994, NOAA-AVHRR studies of vegetation characteristics and deforestation mapping in the Amazon Basis. *Remote Sensing Reviews*, **10,** 5–34.

EITEN, G., 1972, The cerrado vegetation of Brazil. *The Botanical Review*, **38,** 201–341.

FRANÇA, H., 1994, Um estudo fenológico com imagens AVHRR/NOAA nos cerrados do Parque Nacional das Emas, GO. MSc thesis, S. J. Campos, INPE-6120-TDI/581, 96 pp. (in Portuguese).

FRANÇA, H., and SETZER, A. W., 1997, *Regime de queimadas no Parque Nacional das Emas: 1973–95* (FAPESP), 86 pp. (in Portuguese).

GOODLAND, R., 1970, *The Savanna Controversy: Background Information on the Brazilian Cerrado Vegetation*, Savanna Research Series No. 15 (Montreal, Canada: McGill University).

GUTMAN, G. G., 1990, Towards monitoring droughts from space. *Journal of Climate*, **3,** 282–295.

HOLBEN, B. N., SETZER, A., ECK, T. F., PEREIRA, A., SLUTSKER, I., 1996, Effect of dry-season biomass burning on amazon basin aerosol concentration and optical properties, 1992–1994. *Journal of Geophysical Research*, **101**:19, 465–19, 481.

IBGE, 1977–78, Instituto Brasileiro de Geografia e Estatística. Charts SE-22-Y-A-III, SE-22-Y-A-II and SE-22-V-C-VI.

IBAMA, 1989, Instituto Brasileiro do Meio Ambiente e dos Recursos Naturais Renováveis. Unidades de conservação do Brasil. Brasília (in Portuguese).

JUSTICE, C. O., TOWNSHEND, J. R. G., HOLBEN, B. N., and TUCKER, C. J., 1985, Analysis of the phenology of global vegetation using meteorological satellite data. *International Journal of Remote Sensing*, **6,** 1271–1318.

JUSTICE, C. O., and HIERNAUX, P. H. Y., 1986, Monitoring the grasslands of the Sahel using NOAA AVHRR data: Niger 1983. *International Journal of Remote Sensing*, **7,** 1475–1497.

JUSTICE, C. O., HOLBEN, B. N., and GWYNNE, M. D., 1986, Monitoring east African vegetation using AVHRR data. *International Journal of Remote Sensing*, **7,** 1453–1474.

KAUFMAN, Y. J., and REMER, L. A., 1994, Detection of forests using mid-IR reflectance: an application for aerosol studies. *IEEE Transactions on Geoscience and Remote Sensing*, **32,** 672–683.

KIDWELL, K. B., 1990, *Global Vegetation Index: User's Guide*. (Washington, DC: NOAA).

KIDWELL, K. B., 1993, *NOAA Polar Orbits Data: User Guide (Tiros-N, NOAA-6 through NOAA-12)* (Washington, DC: NOAA).

KIMES, D. S., 1983, Dynamics of directional reflectance factor distributions for vegetation canopies. *Applied Optics*, **22,** 1364–1372.

KIMES, D. S., HOLBEN, B. N., and TUCKER, C. J., 1984, Optimal directional view angles for remote sensing. *International Journal of Remote Sensing*, **5,** 887–908.

LIU, W. T., and KOGAN, F. N., 1996, Monitoring regional drought using the Vegetation Condition Index. *International Journal of Remote Sensing*, **17,** 2761–2782.

MALINGREAU, J. P., 1986, Global vegetation dynamics: satellite observations over Asia. *International Journal of Remote Sensing*, **7,** 1121–1146.

NIMER, E., and BRANDÃO, A. M. P. M., 1989, *Balanço hídrico e clima da região dos cerrrados* (Rio de Janeiro: IBGE), 166 pp. (in Portuguese).

PRINCE, S. D., JUSTICE, C. O., and LOS, S. O., 1990, *Remote Sensing of the Sahelian Environment*. (Ispra, Italy: CCE/JRC), 128 pp.

RAMOS-NETO, M. B., and MACHADO, P. C., 1996, O capim flecha (*Tristachya leiostachya* Ness) e sua importância na dinâmica do fogo no Parque Nacional das Emas. *Impactos de queimadas em áreas de cerrado e restinga*, edited by H. S. Miranda, C. H. Saito, and B. F. S. Dias (Brasìl: ECL/UnB), pp. 68–75.

SANTOS, J. R., and SHIMABUKURO, Y. E., 1993, O sensoriamento remoto como indicador das fenofases dos cerrados brasileiros: estudo de caso com dados AVHRR/NOAA. *Simpósio Brasileiro de Sensoriamento Remoto, 7, Curitiba, Maio 10–14, 1993*, vol. 2. (S. J. Campos, INPE), pp. 249–257 (in Portuguese).

SETZER, A. W. and VEERSTRATE, M. M., 1994, Fire and glint in AVHRR's channel 3: a possible reason for the non-saturation mystery. *International Journal of Remote Sensing*, **15,** 711–718.

TUCKER, C. J., and GATLIN, J. A., 1984. Monitoring vegetation in the Nile delta with NOAA-6 and NOAA-7 AVHRR imagery. *Photogrammetric Engineering and Remote Sensing*, **50,** 53–61.

TUCKER, C. J., TOWNSHEND, J. R. G., and GOFF, T. E., 1985, African land-cover classification using satellite data. *Science*, **227,** 369–375.